Temperature and Humidity Profiling in the Arctic Using Ground-Based Millimeter-Wave Radiometry and 1DVAR

Domenico Cimini, Ed R. Westwater, *Fellow, IEEE*, and Albin J. Gasiewski, *Fellow, IEEE*

***Abstract*—A 1-D variational (1DVAR) retrieval technique has been developed for obtaining temperature and humidity profiles from observations of the Ground-Based Scanning Radiometer (GSR) operating at millimeter-wavelengths. The GSR was deployed in two Arctic experiments held at the Atmospheric Radiation Measurement Program in Barrow, Alaska. Temperature and humidity profiles retrieved with the 1DVAR technique are compared with simultaneous radiosonde observations (RAOBs) during the Radiative Heating in Underexplored Bands Campaign (February–March 2007). Examples and statistical results are presented and discussed to demonstrate the achieved retrieval accuracy and vertical resolution. The 1DVAR retrievals based on GSR observations improve the NWP background up to 5 km, particularly in the lower 3 km. The present implementation achieved an root-mean-square (rms) error with respect to RAOB within 1.5 K for temperature and 0.10 g/kg for humidity profiles of up to 5 km in height, with 2.9 and 2.0 degrees of freedom for signal, respectively. Using the interlevel covariance definition of the vertical resolution, the 1DVAR retrievals showed a $<$ 1-km vertical resolution of up to 5 km for both temperature and humidity profiles. The integrated water vapor obtained from the retrieved humidity profiles showed an rms accuracy within 0.10 kg/m^2, with small bias ($<$ 0.01 kg/m^2) and excellent correlation (0.96).**

***Index Terms*—Arctic regions, atmospheric measurements, radiometry.**

I. Introduction

RADIOMETERS operating at millimeter and submillimeter wavelengths show enhanced sensitivity to low water-vapor and liquid contents relative to conventional microwave radiometers that operate below 30 GHz (1 cm) [1], [2]. This sensitivity makes the higher frequency radiometers particularly appealing for accurate observations in the extremely dry and cold conditions typical of the polar regions [1], [3]–[5].

For this reason, the Center for Environmental Research, University of Colorado designed and constructed a 27-channel instrument, called the Ground-Based Scanning Radiometer (GSR), that spans the millimeter- and submillimeter-wave spectrum (from 50 to 400 GHz). The set of frequencies was selected for the simultaneous retrieval of atmospheric temperature and humidity profiles, precipitable water vapor, cloud liquid path, and cloud depolarization ratio [3].

The GSR was first deployed during the Water Vapor Intensive Operational Period (WVIOP, March–April 2004) and, later, during the Radiative Heating in Underexplored Bands Campaign (RHUBC, February–March 2007), both held at the Atmospheric Radiation Measurement (ARM) Program's North Slope of Alaska (NSA) site in Barrow, Alaska [6].

Variational methods have been demonstrated to be well suited for the retrieval of temperature and humidity profiles from ground-based radiometric observations [7]–[9]. In particular, the 1-D variational (1DVAR) technique is an optimal estimation method [10] that combines the observations with a background taken from numerical weather prediction (NWP) model outputs. The assumed error characteristics of both are taken into account [7]. The 1DVAR approach was demonstrated to be advantageous over methods using background from statistical climatology [11]. In fact, as background information, 1DVAR uses a forecast state vector, which is usually more representative of the actual state than a climatologic mean.

In the following sections, we first introduce the experimental setup (Section II). Next, we discuss the 1DVAR retrieval technique developed for GSR to infer temperature and humidity profiles (Section III), and, then, we show results and performances obtained during RHUBC (Section IV).

II. Instrumentation

A. GSR

The GSR is a 27-channel instrument that is able to scan almost continuously from zenith to 3.5 optical air masses on both sides (16.6° to 163.4° elevation) [3]. With respect to conventional instruments working at 20–60 GHz, the contribution by hydrometeor scattering for GSR channels using higher frequencies is, of course, larger. A quantitative analysis of the scattering from nonprecipitating spherical liquid and ice particles for the range of conditions during RHUBC showed that this contribution can be considered within the instrumental-noise level for most, but not all, of the GSR channels [3]. In fact, the scattering contribution becomes significant for higher frequency channels (above 200 GHz). In order to keep the implementation of the 1DVAR technique simple and time effective, we neglect the scattering contribution and, thus, avoid the use

Manuscript received February 3, 2009; revised April 28, 2009 and June 26, 2009. First published October 9, 2009; current version published February 24, 2010. This work was supported in part by the Environmental Sciences Division, U.S. Department of Energy under the Atmospheric Radiation Measurement Program under Grant ER64015 0011106.

D. Cimini is with the Center of Excellence for Remote Sensing and Modeling of Severe Weather, University of L'Aquila, 67100 L'Aquila, Italy (e-mail: nico.cimini@aquila.infn.it).

E. R. Westwater and A. J. Gasiewski are with the Center for Environmental Technology, Department of Electrical and Computer Engineering, University of Colorado at Boulder, Boulder, CO 80309 USA (e-mail: ed.westwater@colorado.edu; al.gasiewski@colorado.edu).

Digital Object Identifier 10.1109/TGRS.2009.2030500

TABLE I
GSR CHANNELS CONSIDERED IN THIS STUDY: NOMINAL AND EQUIVALENT MONOCHROMATIC FREQUENCY. FOR DOUBLE SIDEBAND CHANNELS, THE DISPLACEMENT (Δf) FROM THE LINE CENTER (f_o) IS INDICATED

Channel Number	Frequency	Nominal f_o	Nomina l Δf	EMF f_o	EMF Δf
1	50.300	50.300	0	50.321	0
2	51.760	51.760	0	51.827	0
3	52.625	52.625	0	52.628	0
4	53.290	53.290	0	53.299	0
5	53.845	53.845	0	53.868	0
6	54.400	54.400	0	54.411	0
7	54.950	54.950	0	54.967	0
8	55.520	55.520	0	55.528	0
9	56.025	56.025	0	56.017	0
10	56.215	56.215	0	56.218	0
11	56.325	56.325	0	56.324	0
12	89 V	89.000	0	89.000	0
13	89 H	89.000	0	89.000	0
14	183.31±0.55	183.310	0.550	183.310	0.560
15	183.31±1	183.310	1.000	183.310	1.012
16	183.31±3.05	183.310	3.050	183.310	3.058
17	183.31±4.7	183.310	4.700	183.310	4.612
18	183.31±7	183.310	7.000	183.310	6.952
19	183.31±12	183.310	12.000	183.310	11.880
20	183.31±16	183.310	16.000	183.310	15.776

of higher frequency channels. Consequently, we consider only the 20 lower frequency GSR channels (Table I). These include 11 channels in the low-frequency wing of the 60-GHz oxygen complex, a window channel at 89 GHz and seven channels around the strong 183.31-GHz water-vapor line. Table I also shows the equivalent monochromatic frequency (EMF) [12] that was determined for each GSR channel in order to effectively account for the bandpass; monochromatic brightness-temperature (Tb) calculations at these EMF are within 0.1 K with respect to band-averaged Tb at the conditions encountered during RHUBC. Note that scattering contributions were not considered in the EMF evaluation for the reasons previously discussed.

B. Ancillary Data

In both the WVIOP and RHUBC experiments, the GSR was deployed at the ARM NSA site in Barrow, Alaska. In this paper, information obtained from WVIOP was used to constrain the 1DVAR technique, but retrievals were computed only for RHUBC data. During RHUBC, the GSR joined the resident ARM instrumentation, including a dual-channel microwave radiometer (MWR), a 12-channel MWR profiler (MWRP), a ceilometer, and a meteorological tower measuring *in situ* temperature and humidity at different levels; additionally, two other millimeter-wave radiometers were deployed by ARM, the four-channel GVR and the 15-channel MP-183A [13]. Therefore, we have access to a comprehensive observational and modeling data set for the validation of GSR observations and initialization of GSR retrievals.

C. Radiosondes

At the ARM NSA site, two daily operational radiosondes are launched routinely. During the three weeks of RHUBC, the operational radiosonde observations (RAOBs) were complemented by a large number of additional radiosondes that were released only during clear sky and very low integrated water-vapor content (IWV $\leq$ 2 mm) as detected by near-real-time GSR retrievals [2]. A total of 94 radiosondes were launched during day and night time, of which, 38 were later judged as clear sky according to simultaneous ceilometer data. All radiosondes launched during RHUBC are RS92 manufactured by Vaisala.

III. RETRIEVAL TECHNIQUE

A. 1DVAR

A comparative analysis between a variety of retrieval methods applied to ground-based observations from conventional microwave radiometers (such as MWRP) indicated that the 1DVAR technique outperforms the other considered methods, these being based on various kinds of multiple regression and neural networks [11]. Thus, it seemed convenient to couple the sensitivity of millimeter-wave radiometry with the advantages of the 1DVAR technique for the retrieval of temperature and humidity profiles in the Arctic.

The 1DVAR method developed in this paper builds on earlier work [7]–[9]; the major difference is, indeed, the use of millimeter-wave channels that should improve the accuracy of humidity retrievals in dry conditions. Moreover, multiangle observations are used in the retrieval of both temperature and humidity for improving the vertical resolution and the signal-to-noise ratio. In developing our 1DVAR technique, we follow the standard notation of [14] and indicate with $\mathbf{B}$ and $\mathbf{R}$ the error covariance matrices of the background and observation vector $\mathbf{y}$, respectively. In addition, we indicate the forward-model operator (i.e., radiative transfer model) with $F(\mathbf{x})$. Thus, the technique adjusts the state vector $\mathbf{x}$ from the background state vector $\mathbf{x_b}$ to minimize the following cost function:

$$J = [\mathbf{y} - F(\mathbf{x})]^{\mathrm{T}} \mathbf{R}^{-1} [\mathbf{y} - F(\mathbf{x})] + [\mathbf{x} - \mathbf{x_b}]^{\mathrm{T}} \mathbf{B}^{-1} [\mathbf{x} - \mathbf{x_b}] \quad (1)$$

where $^{\mathrm{T}}$ and $^{-1}$ represent the matrix transpose and inverse, respectively. Note that radiometric noise, representativeness, and forward-model errors all contribute to the observation-error covariance $\mathbf{R}$.

The minimization is achieved using the Levemberg–Marquardt method; this method was found to improve the convergence rate with respect to the classic Gauss–Newton method [7] by introducing a factor γ that is adjusted after each iteration depending on how the cost function J has changed; thus, calling $\mathbf{K}$ the Jacobian matrix of the observation vector with respect to the state vector, the solution

$$\mathbf{x}_{i+1} = \mathbf{x}_i + \left((1+\gamma)\mathbf{B}^{-1} + \mathbf{K}_i^{\mathrm{T}}\mathbf{R}^{-1}\mathbf{K}_i\right)^{-1} \cdot \left[\mathbf{K}_i^{\mathrm{T}}\mathbf{R}^{-1}(\mathbf{y} - F(\mathbf{x}_i)) - \mathbf{B}^{-1}(\mathbf{x}_i - \mathbf{x_b})\right] \quad (2)$$

is iterated until the following convergence criterion is satisfied:

$$[F(\mathbf{x}_{i+1}) - F(\mathbf{x}_i)]^{\mathrm{T}} \mathbf{S}^{-1} [F(\mathbf{x}_{i+1}) - F(\mathbf{x}_i)] \ll n(\mathrm{obs}) \quad (3)$$

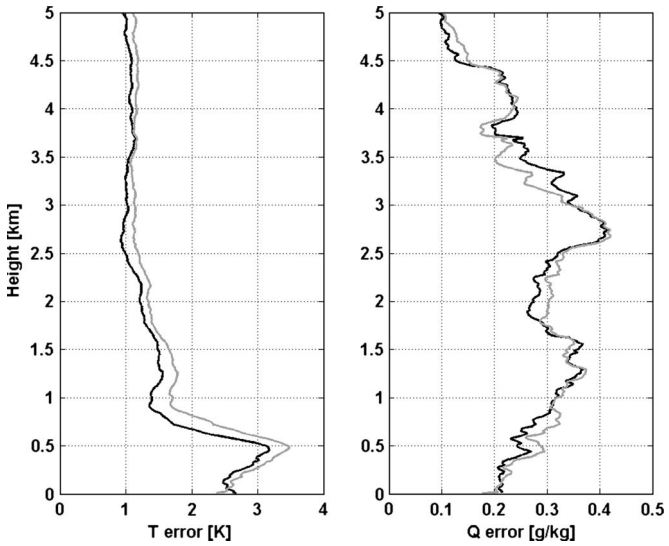

Fig. 1. Diagonal terms (square root) of the background-error covariance matrices $\mathbf{B}$ of (left) temperature and (right) humidity profiles from (gray) ECMWF and (black) NCEP global forecast near the ARM NSA site in Barrow, as computed from 77 forecast-RAOB match ups during the WVIOP 2004.

where

$$\mathbf{S} = \mathbf{R}\left(\mathbf{R} + \mathbf{K}_i \mathbf{B} \mathbf{K}_i^T\right)^{-1} \mathbf{R} \tag{4}$$

and $n(\mathrm{obs})$ indicates the number of observations (i.e., the dimension of $\mathbf{y}$).

B. NWP Model

The 1DVAR technique requires the output of an NWP model as background knowledge of the state vector. For the ARM NSA site, we have access to the output of two NWP models, the European Centre for Medium-scale Weather Forecast (ECMWF) and the National Center for Environmental Prediction (NCEP) global forecast. In Fig. 1, we show the square root of the diagonal terms of the background-error covariance matrices of temperature and humidity profiles from ECMWF and NCEP forecast in Barrow, as computed from a set of simultaneous and colocated forecast-RAOB data collected during the WVIOP. The two models show comparable errors both for temperature and humidity profiles. Therefore, in this paper, we only show retrievals using the background from NCEP global forecast. The NCEP global forecast is initialized every 12 h and released over a 3-h temporal grid and 81 height levels; the levels cover the vertical range from 0 to 20 km, although they are concentrated near the surface.

C. Settings

The state vectors that we used in this study are profiles of temperature and total water (i.e., total of specific humidity and condensed-water content) [15]. As discussed in [7], the choice of total water has the advantages of reducing the dimension of the state vector, enforcing an implicit correlation between humidity and condensed water, including a supersaturation constraint. Moreover, the natural logarithm of total water is used, which creates error characteristics that are more closely Gaussian and prevents unphysical retrieval of negative humidity. The implementation of the natural logarithm of total water within the 1DVAR framework is discussed in the Appendix. The state vectors are given on the same 81 vertical levels defined for the NCEP model, although we perform retrieval just for the levels between 0 and 5 km. Note that the 1DVAR technique applied here is different from that in [7], since it is applied separately for temperature and humidity retrievals. This choice was made for the sake of simplicity of the retrieval algorithm. Since the focus of RHUBC was on IWV, humidity retrievals are desired every time 89- and 183-GHz observations are available, regardless of the functionality of the other GSR channels. This choice gives a larger yield of profile retrievals. In addition, this choice implies fewer constraints for the solution, although we expect it to have a relatively small impact for the conditions during RHUBC.

The background-error covariance matrices $\mathbf{B}$ for both temperature and humidity profiles were computed from a set of 77 simultaneous and colocated forecast-RAOB data (both in clear and cloudy conditions) collected during the WVIOP. While the WVIOP was conducted three years before RHUBC, it was held at the same ARM NSA site during the same season and encountered approximately the same atmospheric conditions; therefore, we consider the WVIOP2004 data to be representative of RHUBC, as well. This calculation of $\mathbf{B}$ inherently includes forecast errors as well as instrumental and representativeness errors from the radiosondes. The radiosonde instrumental error is assumed to be negligible compared with the representativeness error, which consists of the error associated with the representation of volume data (model) with point measurements (radiosondes). The $\mathbf{B}$ matrix including these terms seems appropriate for the radiometric retrieval minimization; since the grid cell of the NWP model is much larger than the radiometer observation volume, the latter can be assumed as a point measurement compared with the model cell, similar to radiosondes. Note that we assumed the $\mathbf{B}$ matrix estimated for humidity to be valid for our control variable total water, since no information on the background cloud-water error covariance was available to us. This assumption is strictly valid during clear sky conditions only, while it underestimates the background error in cloudy conditions. The implications are that, under cloudy conditions, our humidity retrieval would rely more on the background and less on measurements than would be possible by adopting a $\mathbf{B}$ matrix that includes both humidity and liquid-water errors. However, considering the infrequent and optically thin cloudy conditions encountered during RHUBC, we believe this assumption does not affect our results significantly.

The observation vector is defined as the vector of Tb measured by GSR at a number of elevation angles, plus the surface temperature and humidity given by the sensors mounted on the lowest level (2 m) of the meteorological tower. The observation-error covariance matrix $\mathbf{R}$ was estimated using the GSR data taken from the WVIOP, following the approach in [7]. The forward model $F(\mathbf{x})$ is provided by the NOAA microwave radiative-transfer code [16], which also provides the weighting functions that we use to compute the Jacobians $\mathbf{K}$ with respect to temperature, humidity, and liquid water. The forward

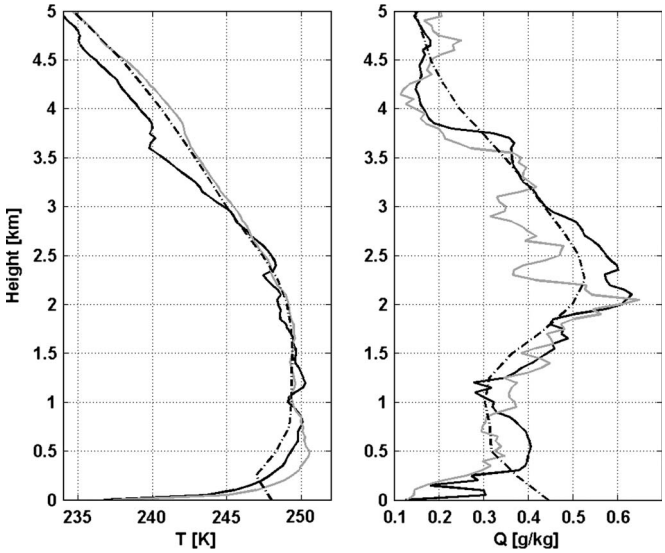

Fig. 2. Typical example of (in gray) 1DVAR retrievals compared with the background from (black dashed) NWP and (black solid) RAOB temperature and humidity profiles (RAOB launched at 16:24 March 11, 2007).

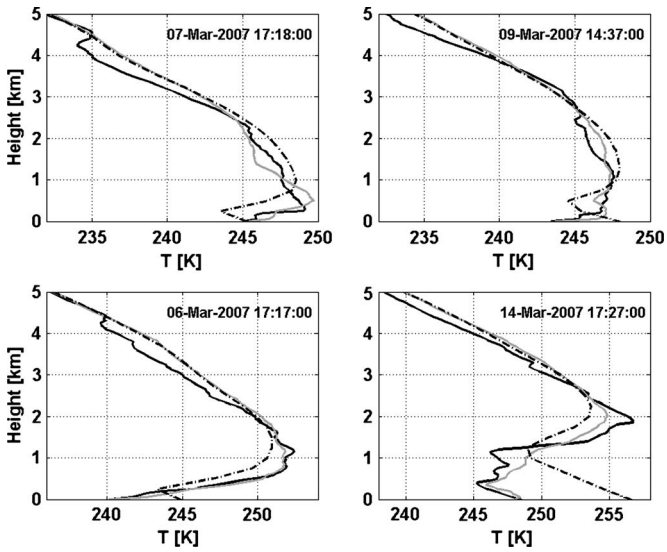

Fig. 3. More examples of (black dashed) background and (gray) 1DVAR temperature retrievals versus (black solid) RAOB temperature profiles.

model was run at the GSR EMF given in Table I; typical errors with respect to band-averaged Tb are within 0.1 K and were accounted for in the forward-modeling component of the observation error.

The number of channels and elevation angles actually used was selected as a tradeoff between the number of forward-model computations and the expected vertical resolution, expressed as the number of layers that are retrieved independently, i.e., the degrees of freedom for signal (DFS) [10]. For example, using the full set of oxygen channels (11) and elevation angles (72) for the retrieval of temperature profiles would require 792 runs of the forward model $F(\mathbf{x})$ per iteration. This selection, which is surely not the most effective, would provide slightly more than four DFS. On the other hand, using just one channel with all elevation angles would require 72 runs and provide about 2.7 DFS. The tradeoff was chosen at six channels (54.4 to 56.325 GHz) and six elevation angles (corresponding to 1.0 to 3.5, with 0.5-step optical air masses); this setting requires 36 runs of $F(\mathbf{x})$ per iteration and provides 2.9 DFS. Similarly, for the humidity retrieval we choose eight channels (89 to 183 ± 16 GHz) and two angles (1.0 and 1.5 optical air masses), requiring 16 runs of $F(\mathbf{x})$ per iteration and providing 2.0 DFS. Note that, since the DFS depend on the atmospheric state, these considerations strictly apply for the dry conditions typical of polar winters only.

IV. Results

The 1DVAR retrieval technique and the settings described in the previous section were applied to GSR data collected during the three-week duration of RHUBC. These observations were found to be consistent with simultaneous and colocated observations from the other two independent 183-GHz radiometers and with simulations obtained from RAOBs [13], generally within the expected accuracy. A typical example of temperature and humidity retrieved profiles is illustrated in Fig. 2, obtained from the GSR brightness temperatures observed within 10 min from the radiosonde launch time. As a comparison, we also show the background NWP profiles that were used as a first guess and the *in situ* observations from the radiosonde.

Concerning the temperature profile, we note that in this case, the NWP forecast is in good agreement with the RAOB, particularly in the atmospheric layer from 0.5 to 3.0 km. Conversely, in the upper part of the vertical domain (3–5 km), the NWP forecast shows about 1–2-K bias with respect to the RAOB, while in the very first layer (0–0.5 km), it differs from RAOB by more than 10 K. Conversely, the 1DVAR retrieval agrees better with the RAOB in the lowest levels, while for the upper levels, the retrieved temperature tends to lie over the NWP background. These considerations are consistent with the diagonal terms of the background-error covariance matrix in Fig. 1 and with the exponential-like decay of the temperature Jacobian [1], [7] with height, which suggests that the contribution of the ground-based radiometric observations is mostly concentrated in the first few kilometers.

As for the humidity, again we note that the NWP forecast captures well the vertical structure, although with lower resolution, except for the first 500 m, where the 1DVAR retrieval shows a much better agreement with the RAOB. However, considering the NWP error analysis in Fig. 1 and that the humidity Jacobians of 183-GHz channels are relatively smooth with respect to height [1], [2], it is reasonable that the retrieved humidity departs from the background throughout the vertical domain.

Similar considerations apply for other cases shown in Fig. 3 (temperature) and Fig. 4 (humidity). The statistical comparison of background and retrievals versus RAOB resulted in the bias and standard deviation (std) shown in Fig. 5. We note that, in general, the retrieved profiles show agreement with RAOB better than the background for both temperature and humidity. This demonstrates the benefit of adding ground-based observations to the forecast, as one would expect. For temperature retrievals, both bias and std are within 1 K up to 5 km. For humidity profiles, the bias is within 0.05 g/kg up to 5 km, while

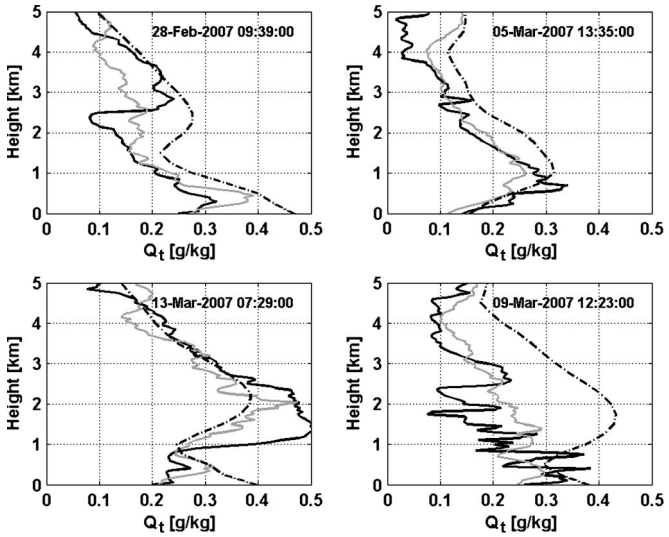

Fig. 4. More examples of (black dashed) background and (gray) 1DVAR humidity retrievals versus (black solid) RAOB specific-humidity profiles. Note that for the case of March 13, 2007, the 1DVAR technique estimated a cloud from (black dotted) 0.5–1 km.

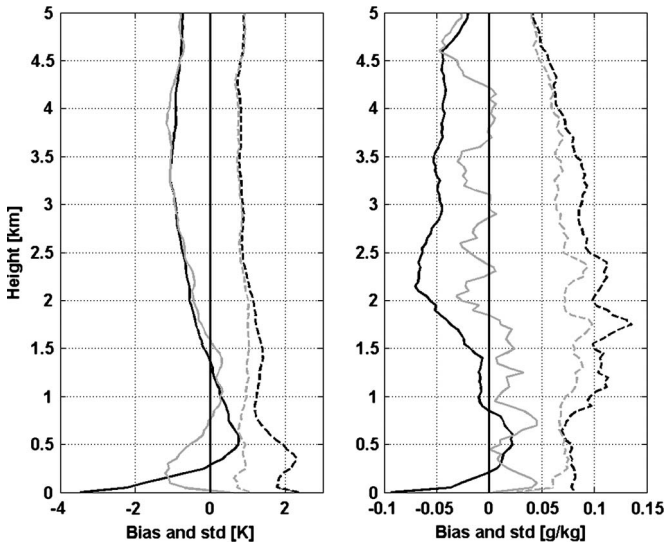

Fig. 5. Profiles of (solid) bias and (dashed) std of (black) background and (gray) 1DVAR retrievals with respect to RAOB for (left) temperature and (right) humidity. The set of 94 RAOBs launched during RHUBC is used here.

the std reaches a maximum of 0.08 g/kg at about 2.5 km. The corresponding root-mean-square (rms) error for temperature and humidity profiles are shown in Fig. 6 for both background and retrievals. In addition, Fig. 6 shows the rms error of retrievals obtained using surface temperature and humidity only, i.e., without radiometric observations. Therefore, the rms error reduction of 1DVAR retrievals with respect to 1) background and 2) to background plus surface measurements demonstrate the benefit of adding radiometric observations to 1) the forecast and 2) to the forecast coupled with surface temperature and humidity sensors only.

In summary, the 1DVAR retrieval rms error with respect to RAOB remains within 1.5 K for temperature and 0.10 g/kg for humidity. These results are similar to those of [11] (using a 12-channel MWRP from 20 to 60 GHz) and of [5] (using

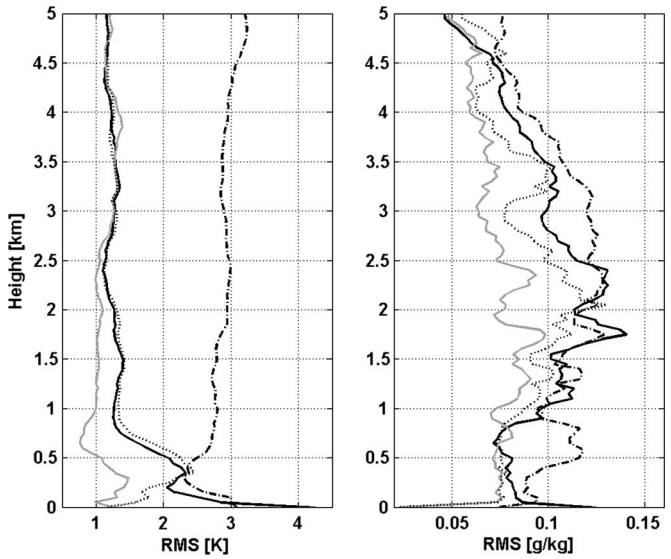

Fig. 6. Profiles of (solid) rms error of (black) background and (gray) 1DVAR retrievals with respect to RAOB for (left) temperature and (right) humidity. The dotted line indicates the rms error of retrievals obtained coupling the background with surface temperature and humidity only. The dashed-dotted line indicates the variability (in terms of std) of the 94-RAOB set launched during RHUBC.

multivariate quadratic regression applied to observations from a 14-channel 51–190-GHz radiometer in a mountain site).

Considering just the retrievals computed at the time of radiosonde ascents (total of 94 RAOBs), the convergence rate was 100% for both temperature and total water. The solution usually takes three to ten iterations to converge; note that using the classic Gauss–Newton method and limiting to a maximum of ten iterations, just 80% of the total-water retrievals would reach convergence.

Another important aspect of the retrievals' performance is the achieved vertical resolution. However, there are different definitions for its quantitative evaluation. One robust definition of the vertical resolution is the inverse of diagonal of the averaging kernel matrix (AKM) [10], scaled by the layer spacing. Using the AKM definition, the vertical resolution of 1DVAR temperature retrievals degrades roughly linearly with height, from a few hundreds of meters near the surface to $\sim$10 km at 5 km height; for humidity profiles, the vertical resolution degrades roughly linearly with height, from a few hundreds of meters near the surface to $\sim$4 km at 4 km height and degrades much more rapidly above that. However, the AKM definition is conservative because only the Tb information is used and not that of the initial guess. If the forecast is regarded as a pseudomeasurement, then a more representative resolution definition is obtained. For example, more optimistic results are given by another definition of vertical resolution relying on the interlevel-covariance method [17], [18]. Using the interlevel-covariance definition, the vertical resolution for 1DVAR temperature retrievals degrades roughly linearly with height, from 50 m near the surface to 1 km at 1.5 km height, and remains within $\sim$1 up to 5 km; for humidity retrievals, the resolution slowly degrades with height, from a few hundreds of meters near the surface to $\sim$1 km at 5 km height. These results are consistent with those of [11] (using 1DVAR with

a 12-channel MWRP from 20–60 GHz) and of [18] (combining retrievals from satellite and a ground-based 12-channel 20–60-GHz MWRP).

Finally, we also checked the 1DVAR retrieval performances for IWV, by comparing the IWV values computed from background and retrieved humidity profiles with the ones obtained from RAOBs. Although the background provides already an excellent accuracy (0.27 kg/m^2) and good correlation (0.78) with respect to RAOBs, the retrieved values add a substantial improvement to the accuracy (0.10 kg/m^2) with a small bias (less than 0.01 kg/m^2) and excellent correlation (0.96). This level of accuracy is consistent with the findings in [19], processing GSR 89 and 183-GHz data with a piecewise linear-regression method. This confirms the impression in [7] that the 1DVAR technique does not need an additional constraint to force the IWV to match that retrieved by a simpler method, as this is achieved implicitly in the 1DVAR approach. Although it would have been ideal to compare the temperature and humidity profiling performances obtained with our approach with those obtained operationally by ARM (based on MWRP observations), this was not possible for RHUBC since the MWRP suffered from malfunctions during a large part of the experiment.

V. Conclusion and Further Work

A 1DVAR retrieval technique has been developed to combine in an optimal way ground-based millimeter-wavelength scanning radiometric observations with the background from an NWP model. The 1DVAR technique has been used to retrieve profiles of temperature, humidity, and liquid-water content (through the control variable total water) during an experiment focusing on extremely dry conditions (RHUBC), held at the ARM NSA site in Barrow, Alaska.

Error analysis has shown that the 1DVAR retrievals based on GSR observations improves the NWP background up to 5 km, particularly in the lower 3 km. With the present implementation, we achieved an rms error with respect to RAOB within 1.5 K for temperature and 0.10 g/kg for humidity profiles up to 5 km height, with 2.9 and 2.0 DFS for signal, respectively. Using the interlevel-covariance definition of the vertical resolution, our 1DVAR retrievals show vertical resolution within 1 up to 5 km for both temperature and humidity profiles. Finally, water-vapor burden obtained by integrating the retrieved humidity profiles showed rms accuracy with respect to that obtained by RAOBs within 0.10 kg/m^2, with small bias (less than 0.01 kg/m^2) and excellent correlation (0.96), leading to a substantial improvement with respect to the NWP background. Therefore, statistics of 1DVAR retrievals based on GSR data during RHUBC confirm the theoretical expectations for accuracy and vertical resolution, which outperform results from other methods taking their background from statistical climatology.

The 1DVAR method is flexible and suitable for data assimilation in NWP models. The method may be adapted for running operationally at ARM sites and providing a new value-added product. Future work may be dedicated to implementing the 1DVAR technique to exploit the full spectral and angular GSR potential and extending the retrieval scheme to include observations from other passive (as MP-183A, MWRP, ...) and active (cloud radar, radar-wind profiler, ...) instruments to develop an integrated modular system for tropospheric profiling.

Appendix
Implementation of Total Water Within 1DVAR

In this paper, we follow the approach of [7] (and references therein) for implementing the total-water retrievals within the 1DVAR technique. Hereafter we summarize the main relationships we have adopted.

The humidity components of the state vector are defined as the natural logarithm of total water, i.e., $\ln q_t = \ln(q + q_c)$, where q is the specific humidity and q_c is the condensed-water content (liquid and ice), both in [gram per kilogram]. The advantages of this choice are discussed within the text. This control variable utilizes a smooth transfer function for partitioning vapor and condensed water that provides continuous derivative throughout the relative-humidity range, avoiding discontinuities that may produce unstable iterations when the humidity is close to the saturation value. The condensed part of the total water is further partitioned between liquid and ice fractions, assuming a linear dependence on air temperature T. Calling q_l and q_i the liquid and ice water contents, then $q_c = f_l \cdot q_l + (1 - f_l) \cdot q_i$, where f_l assumes the value zero, $(T + 40)/40$, or one when $T < -40$ °C, $-40° < T < 0$ °C, or $T > 0$ °C, respectively. The ice fraction is ignored in the forward model, as it is assumed to have negligible extinction for the channels used here.

Calling $q_{\rm sat}$ the saturation value of q, $RHq_t = q_t/q_{\rm sat}$, the transfer function is such that we have three cases, shown at the bottom of the page, where RH_1 and RH_2 are two arbitrary thresholds, $\alpha = (\pi/2)((RHq_t - RH_2)/(RH_2 - RH_1))$, while c_1, and c_2 are the coefficients enforcing continuity, i.e., $c_1 = (q_{\rm sat}/\pi)(RH_2 - RH_1)$ and $c_2 = (q_{\rm sat}/2)(RH_2 - RH_1)|_{RHq_t \equiv RH_2}$.

Thus, if $RHq_t <= RH_1$ (case 1), total water consists of specific humidity only (no liquid/ice), while if $RHq_t >= RH_2$

Case	If	Then	Then
1	$RHq_t <= RH_1$	$dq_c/dq_t = 0$	$q_c = 0; \quad q_t = q$
2	$RH_1 < RHq_t < RH_2$	$dq_c/dq_t = \cos^2\alpha$	$q_c = c_1 \cdot (\sin\alpha \cdot \cos\alpha + \alpha) + c_2; \quad q = q_t - q_c$
3	$RHq_t >= RH_2$	$dq_c/dq_t = 1$	$q_c = q_t - q_{\rm sat}; \quad q = q_{\rm sat}$

(case 2), the humidity is saturated, and any additional total water contributes entirely to condensed-water content. For the intermediate situation (case 3), $RH_1 < RHq_t < RH_2$ and vapor and condensed water are calculated using $q = q_t - q_c$, and $q_c = c_1 * (\sin\alpha\cos\alpha + \alpha) + c_2$, respectively.

Calling Jq and Jq_l the brightness temperature Jacobians with respect to specific humidity and liquid water content ($Jq = \delta\mathrm{Tb}/\delta q$, and $Jq_l = \delta\mathrm{Tb}/\delta q_l$), the Jacobian for the state variable $\ln q_t = \ln(q + q_c)$, i.e., $J \ln q_t = \delta\mathrm{Tb}/\delta(\ln q_t)$, in the aforementioned three cases is

Case	Jacobian with respect to $\ln q_t$
1	$J \ln q_t = q \cdot Jq$
2	$J \ln q_t = q_t \cdot (Jq \cdot \sin^2\alpha + 1/f_1 \cdot Jq_1 \cdot \cos^2\alpha)$
3	$J \ln q_t = q_t \cdot Jq_1 \cdot 1/f_1$

Note that the two arbitrary threshold values RH_1 and RH_2 were 0.9 and 1.1, respectively, in [7], while they were set to 0.8 and 1.1 in this paper to allow condensed-water formation at lower relative humidity values.

ACKNOWLEDGMENT

The authors would like to thank Dr. M. Klein and Dr. V. Leuski for help in developing the GSR data that were used in our analysis. D. Cimini would like to thank the Fondazione Ugo Bordoni for receiving the Prof. D'Auria Award for the best presentation in Atmospheric Topics at the Microrad 2008 meeting in which the results in this paper were shown. The authors dedicate this paper to the many that have lost lives and beloved ones during the April 6, 2009 earthquake in L'Aquila. May peace be with them.

REFERENCES

[1] P. E. Racette, E. R. Westwater, Y. Han, A. J. Gasiewski, M. Klein, D. Cimini, D. C. Jones, W. Manning, E. J. Kim, J. R. Wang, V. Leuski, and P. Kiedron, "Measuring low amounts of precipitable water vapor using millimeter-wave radiometry," *J. Atmos. Ocean. Technol.*, vol. 22, no. 4, pp. 317–337, Apr. 2005.

[2] D. Cimini, E. R. Westwater, A. J. Gasiewski, M. Klein, V. Y. Leuski, and J. C. Liljegren, "Ground-based millimeter- and submillimeter-wave observations of low vapor and liquid water contents," *IEEE Trans. Geosci. Remote Sens.*, vol. 45, no. 7, pp. 2169–2180, Jul. 2007.

[3] D. Cimini, E. R. Westwater, A. J. Gasiewski, M. Klein, V. Y. Leuski, and S. G. Dowlatshahi, "The ground-based scanning radiometer: A powerful tool for study of the Arctic atmosphere," *IEEE Trans. Geosci. Remote Sens.*, vol. 45, no. 9, pp. 2759–2777, Sep. 2007.

[4] M. P. Cadeddu, J. C. Liljegren, and A. L. Pazmany, "Measurements and retrievals from a new 183-GHz water-vapor radiometer in the Arctic," *IEEE Trans. Geosci. Remote Sens.*, vol. 45, no. 7, pp. 2207–2215, Jul. 2007.

[5] P. Ricaud, B. Gabard, S. Derrien, J.-P. Chaboureau, T. Rose, A. Mombauer, and H. Czekala, "HAMSTRAD-Tropo, a 183-GHz radiometer dedicated to sound tropospheric water vapor over Concordia Station, Antarctica," *IEEE Trans. Geosci. Remote Sens.*, 2009, to be published.

[6] T. P. Ackerman and G. M. Stokes, "The atmospheric radiation measurement program," *Phys. Today*, vol. 56, no. 1, pp. 38–44, Jan. 2003.

[7] T. Hewison, "1D-VAR retrievals of temperature and humidity profiles from a ground-based microwave radiometer," *IEEE Trans. Geosci. Remote Sens.*, vol. 45, no. 7, pp. 2163–2168, Jul. 2007.

[8] U. Löhnert, S. Crewell, and C. Simmer, "An integrated approach toward retrieving physically consistent profiles of temperature, humidity, and cloud liquid water," *J. Appl. Meteorol.*, vol. 43, no. 9, pp. 1295–1307, Sep. 2004.

[9] U. Löhnert, E. van Meijgaard, H. K. Baltink, S. Groß, and R. Boers, "Accuracy assessment of an integrated profiling technique for operationally deriving profiles of temperature, humidity and cloud liquid water," *J. Geophys. Res.*, vol. 112, no. D4, p. D04 205, 2007.

[10] C. D. Rodgers, *Inverse Methods for Atmospheric Sounding: Theory and Practice*. Singapore: World Scientific, 2000.

[11] D. Cimini, T. J. Hewison, L. Martin, J. Güldner, C. Gaffard, and F. S. Marzano, "Temperature and humidity profile retrievals from ground-based microwave radiometers during TUC," *Meteorol. Z.*, vol. 15, no. 5, pp. 45–56, Feb. 2006.

[12] D. Cimini, T. J. Hewison, and L. Martin, "Comparison of brightness temperatures observed from ground-based microwave radiometers during TUC," *Meteorol. Z.*, vol. 15, no. 1, pp. 19–25, Feb. 2006.

[13] D. Cimini, F. Nasir, E. R. Westwater, V. H. Payne, D. D. Turner, E. J. Mlawer, M. L. Exner, and M. P. Cadeddu, "Comparison of ground-based millimeter-wave observations and simulations in the Arctic winter," *IEEE Trans. Geosci. Remote Sens.*, vol. 47, no. 9, pp. 3098–3106, Sep. 2009.

[14] K. Ide, P. Courtier, M. Ghil, and A. C. Lorenc, "Unified notation for data assimilation: Operational, sequential, and variational," *J. Meteorol. Soc. Jpn.*, vol. 75, no. 1B, pp. 181–189, 1997.

[15] G. Deblonde and S. English, "One-dimensional variational retrievals for SSMIS simulated observations," *J. Appl. Meteorol.*, vol. 42, no. 10, pp. 1406–1420, Oct. 2003.

[16] J. A. Schroeder and E. R. Westwater, "User's guide to WPL microwave radiative transfer software," Nat. Ocean. Atmos. Admin., Boulder, CO, NOAA Technical Memorandum, ERL WPL-213, 1991.

[17] W. L. Smith, W. F. Feltz, R. O. Knuteson, H. E. Revercomb, H. M. Woolf, and H. B. Howell, "The retrieval of planetary boundary layer structure using ground-based infrared spectral radiance measurements," *J. Atmos. Ocean. Technol.*, vol. 16, no. 3, pp. 323–333, Mar. 1999.

[18] J. C. Liljegren, S. A. Boukabara, K. Cady-Pereira, and S. A. Clough, "The effect of the half-width of the 22-GHz water vapor line on retrievals of temperature and water vapor profiles with a twelve-channel microwave radiometer," *IEEE Trans. Geosci. Remote Sens.*, vol. 43, no. 5, pp. 1102–1108, May 2005.

[19] E. R. Westwater, D. Cimini, V. Mattioli, A. J. Gasiewski, M. Klein, V. Leuski, and D. D. Turner, "Deployments of microwave and millimeterwave radiometers in the Arctic," in *Proc. MicroRad*, 2008, pp. 1–4.

Domenico Cimini received the Laurea (*cum laude*) and Ph.D. degrees in physics from the University of L'Aquila, L'Aquila, Italy, in 1998 and 2002, respectively.

From 2002 to 2004, he was with the Center of Excellence for Remote Sensing and Modeling of Severe Weather (CETEMPS), University of L'Aquila, L'Aquila, Italy. From 2004 to 2005, he was a Visiting Fellow with the Cooperative Institute for Research in Environmental Sciences, University of Colorado at Boulder. From 2005 to 2006, he was with the Institute of Methodologies for the Environmental Analysis of the Italian National Research Council, working on ground- and satellite-based observations of cloud properties. In 2006, he was an Affiliate with the Center for Environmental Technology, Department of Electrical and Computer Engineering, University of Colorado at Boulder, where he served as Adjunct Professor in 2007. He is currently a Researcher at CETEMPS, working on ground- and satellite-based passive microwave and infrared radiometry.

Dr. Cimini was the recipient of the *Fondazione Ugo Bordoni Award* 2008 in memory of Prof. Giovanni D'Auria.

Ed R. Westwater (SM'91–F'01) received the B.A. degree in physics and mathematics from the Western State College of Colorado, Gunnison, in 1959, and the M.S. and Ph.D. degrees in physics from the University of Colorado at Boulder (CU-Boulder), in 1962 and 1970, respectively.

From 1960 to 1995, he was with the U.S. Department of Commerce. He is currently a Research Professor with the National Oceanic Atmospheric Administration–Center for Environmental Technology (CET) and the Cooperative Institute for Research in Environmental Science (CIRES), Department of Electrical and Computer Engineering (ECE), CU-Boulder, where, since 1995, he has been with CIRES and, since 2006, with CET/ECE. His research has been concerned with microwave absorption in the atmosphere, remote sensing of the atmosphere and ocean surface, microwave and infrared radiative transfer, ground- and satellite-based remote sensing by passive radiometry, and the application of mathematical inversion techniques to problems in remote sensing. He has authored or coauthored more than 290 publications.

Dr. Westwater is a member of the American Meteorological Society, American Geophysical Union, and Mathematical Association of America. He was the Chairman and Organizer of the 1992 International Specialists Meeting on Microwave Radiometry and Remote Sensing Applications (MicroRad'1992) and was a Coorganizer of the MicroRad'2001. He is the past Chairman of the International Union of Radio Science Commission F from 2000 to 2002. He served as Associate Editor of *Radio Science* from 1999 to 2002. He is currently an Associate Editor of the IEEE TRANSACTIONS ON GEOSCIENCE AND REMOTE SENSING (TGARS) and served as a Guest Editor of the TGARS Special Issue devoted to MicroRad'2004, MicroRad'2006, and MicroRad 2008. He presented the American Meteorological Society's Remote Sensing Lecture in 1997 (elected December 3, 2000). He was the recipient of the 2003 Distinguished Achievement Award from the IEEE Geoscience and Remote Sensing Society. He was the recipient of the 15th V. Vaisala Award from the World Meteorological Society in 2001.

Albin J. Gasiewski (SM'81–M'88–SM'95–F'02) received the M.S. and B.S. degrees in electrical engineering and the B.S. degree in mathematics from Case Western Reserve University, Cleveland, OH, in 1983 and the Ph.D. degree in electrical engineering and computer science from the Massachusetts Institute of Technology, Cambridge, in 1989.

From 1989 to 1997, he was a Faculty Member with the School of Electrical and Computer Engineering, Georgia Institute of Technology, Atlanta, where he became an Associate Professor. He has developed and taught courses on electromagnetics, remote sensing, instrumentation, and wave propagation theory. From 1997 to 2005, he was with the U.S. National Oceanic and Atmospheric Administration's Environmental Technology Laboratory (ETL), Boulder, CO, where he was Chief of ETL's Microwave Systems Development Division. He is currently a Professor of electrical and computer engineering with the University of Colorado at Boulder (CU-Boulder) and Director of the CU-Boulder Center for Environmental Technology. His technical interests include passive and active remote sensing, radiative transfer, antennas and microwave circuits, electronic instrumentation, meteorology, and oceanography.

Prof. Gasiewski is past President (2004–2005) of the IEEE Geoscience and Remote Sensing Society (GRSS). He is a member of the American Meteorological Society, the American Geophysical Union, the International Union of Radio Scientists (URSI), Tau Beta Pi, and Sigma Xi. He currently serves as Vice Chair of U.S. National Committee/URSI Commission F. He served on the U.S. National Research Council's Committee on Radio Frequencies from 1989 to 1995. He was the General Cochair of the 2006 International Geoscience and Remote Sensing Symposium, Denver, CO, and a recipient of the 2006 Outstanding Service Award from the GRSS.